

Upregulation of the Mammalian Target of Rapamycin Complex 1 Pathway by Ras Homolog Enriched in Brain in Pancreatic β -Cells Leads to Increased β -Cell Mass and Prevention of Hyperglycemia

Suirin Hamada,¹ Kenta Hara,¹ Takeshi Hamada,¹ Hisafumi Yasuda,¹ Hiroaki Moriyama,¹ Rika Nakayama,² Masao Nagata,¹ and Koichi Yokono¹

OBJECTIVE—Components of insulin/IGF-1 receptor-mediated signaling pathways in pancreatic β -cells have been implicated in the development of diabetes, in part through the regulation of β -cell mass in vivo. Studies in vitro have shown that the protein Ras homolog enriched in brain (Rheb) plays a key role as a positive upstream regulator of the mammalian target of rapamycin complex 1 (mTORC1) pathway in integrating inputs from nutrients and growth factors for cell growth. Our objective was to investigate the role of the mTORC1 pathway in the regulation of β -cell mass in vivo.

RESEARCH DESIGN AND METHODS—We generated transgenic mice that overexpress Rheb in β -cells. We examined the activation of the mTORC1 pathway and its effects on β -cell mass, on glucose metabolism, and on protection against hyperglycemia.

RESULTS—Immunoblots of islet extracts revealed that the phosphorylation levels of ribosomal protein S6 and eukaryotic initiation factor 4E binding protein 1, downstream effectors for mTORC1, were upregulated in transgenic β -cells. Immunostaining of the pancreatic sections with anti-phospho-S6 antibody confirmed upregulation of the mTORC1 pathway in β -cells in vivo. The mice showed improved glucose tolerance with higher insulin secretion. This arose from increased β -cell mass accompanied by increased cell size. The mice also exhibited resistance to hyperglycemia induced by streptozotocin and obesity.

CONCLUSIONS—Activation of the mTORC1 pathway by Rheb led to increased β -cell mass in this mouse model without producing obvious unfavorable effects, giving a potential approach for the treatment of β -cell failure and diabetes. *Diabetes* 58:1321–1332, 2009

D diabetes arises from the relative failure of β -cells to secrete sufficient insulin to maintain normal metabolism (1). Under insulin-resistant conditions such as obesity, blood glucose levels are maintained within a normal range if the β -cells can compensate for the increased demand. This compensatory mechanism is acquired by an increase in β -cell mass

through augmentation of islet neogenesis and replication, by hypertrophy, and by a reduction in the rate of β -cell death (2).

A number of studies have indicated that insulin and IGF-1 receptor-mediated signaling pathways are involved in the regulation of β -cell mass (3–11). Activation of the insulin or IGF-1 receptors induces tyrosine phosphorylation of insulin receptor substrates (IRSs), which recruit several signal intermediates, including phosphoinositide-3 kinase. Phosphoinositide-3 kinase phosphorylates inositol phospholipids, which then activates 3'-phosphoinositide-dependent kinase 1, which directly phosphorylates and activates p70 S6 kinase and protein kinase B (PKB) synergistically with mammalian target of rapamycin (mTOR) (12–14). Ribosomal protein S6 and the transcription factor forkhead box O1 (FoxO1), substrates of p70 S6 kinase (p70S6K) and PKB, respectively, are also implicated in this process (15–17).

The Ser/Thr protein kinase mTOR signals through two physically distinct multiprotein complexes called mTOR complex (mTORC) 1 and 2 (12). mTORC1 contains the polypeptides raptor and mLST8, and the ability of raptor to present its substrates properly to the mTOR catalytic domain is essential for the regulation of the translational regulators eukaryotic initiation factor 4E binding protein 1 (4EBP1) and p70S6K (18,19). The proximal regulator of mTORC1 is a Ras-like small GTPase named Ras homolog enriched in brain (Rheb) (20,21). Rheb binds directly to the mTOR catalytic domain and activates it in a manner dependent on the state of Rheb nucleotide charging (22). Insulin or IGF-1 enhances Rheb GTP charging via inhibition of the GTPase activating function of the product of the tuberous sclerosis (TSC) genes, the TSC1–TSC2 heterodimer (23–31). The mTORC1 pathway is also regulated by nutrients (32). Whereas amino acid depletion interferes with the ability of Rheb to enable mTORC1 to attain an active configuration, glucose depletion reduces Rheb GTP charging through the ability of the AMP-activated kinase to phosphorylate TSC2 and to direct its GTPase-activating activity toward Rheb (33,34). FKBP38 (FK506-binding protein 38) is also an endogenous inhibitor of mTOR whose inhibitory activity is antagonized by Rheb in response to growth factors and nutrient availability (35).

To investigate the metabolic role of the mTOR signaling pathway in a mammalian model, we created transgenic mice with an overproduction of Rheb in pancreatic β -cells. These mice exhibited increased insulin secretion in response to glucose loading and resistance to streptozotocin

From the ¹Department of Internal and Geriatric Medicine, Kobe University Graduate School of Medicine, Kobe, Japan; and the ²Laboratory for Animal Resources and Genetic Engineering, Center for Developmental Biology (CDB), RIKEN, Kobe, Japan.

Corresponding author: Kenta Hara, harak@kobe-u.ac.jp.

Received 18 April 2008 and accepted 25 February 2009.

Published ahead of print at <http://diabetes.diabetesjournals.org> on 3 March 2009. DOI: 10.2337/db08-0519.

© 2009 by the American Diabetes Association. Readers may use this article as long as the work is properly cited, the use is educational and not for profit, and the work is not altered. See <http://creativecommons.org/licenses/by-nc-nd/3.0/> for details.

The costs of publication of this article were defrayed in part by the payment of page charges. This article must therefore be hereby marked "advertisement" in accordance with 18 U.S.C. Section 1734 solely to indicate this fact.

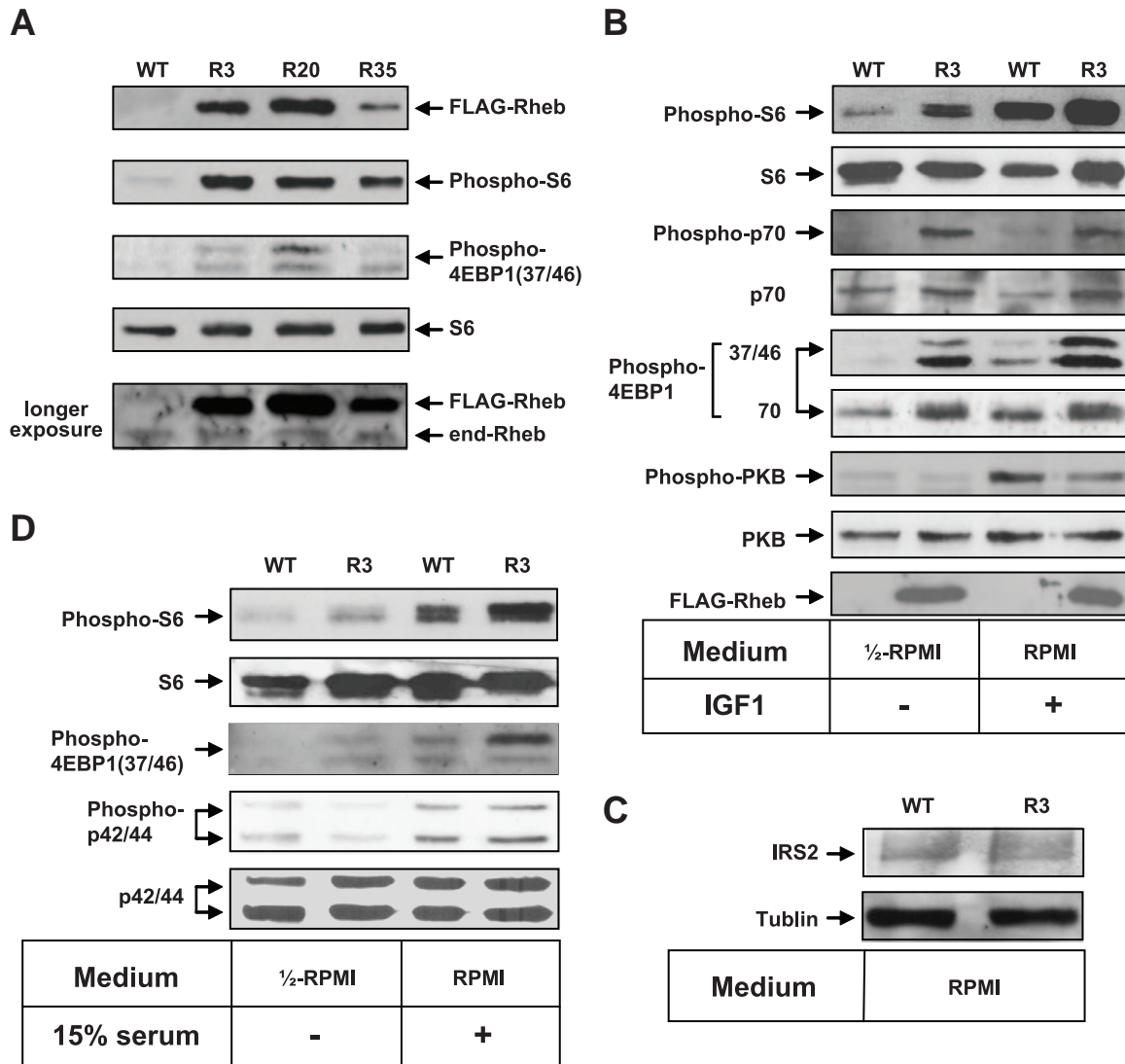


FIG. 1. Activation of the mTORC1 pathway by overexpression of FLAG-Rheb in pancreatic β -cells. Islets isolated from mice of each genotype were incubated either in 50% RPMI medium without FCS (A, B, and D) or in RPMI medium (C), or they were stimulated with 100 nmol/l IGF-1 (B) or 15% FCS (D) as indicated. The same amounts of cellular extracts were analyzed by immunoblotting with the antibodies to Rheb, phospho-S6 ribosomal protein (Ser235/236), S6 ribosomal protein, phospho-4EBP1 (Thr37/46 or Thr70), phospho-p70 S6 kinase (Thr389), p70 S6 kinase, phospho-PKB (Ser473), PKB, phospho-p44/42 MAP kinase (Thr202/Tyr204), p44/42 MAP kinase, or IRS2. A representative experiment is shown. The bottom panel in A shows the same blot as the top panel, except that it was exposed longer to detect the endogenous Rheb (end-Rheb). E: Relative quantification of phospho-S6 (Ser235/236), phospho-4EBP1 (T37/46 or T70), phospho-PKB (Ser473), phospho-p44/42 MAP kinase (Thr202/Tyr204), and IRS2. The immunoblots were scanned, and the optical density for R3 with IGF1 or FCS stimulation (A, B, and D) or the optical density for R3 (C) was set to 100%. F: Immunoprecipitation with the anti-FLAG antibody was performed using lysates of the hypothalamus, muscle, or liver isolated from mice of each genotype and analyzed by immunoblotting with the same antibody. WT, wild type.

cin- and obesity-induced hyperglycemia, which were accompanied by increased β -cell mass.

RESEARCH DESIGN AND METHODS

A wild-type human *Rheb* gene tagged with a FLAG sequence at the NH₂-terminus was introduced downstream of the rat insulin promoter. The transgene was microinjected into pronuclei of C57BL/6N zygotes. Mice carrying the lethal yellow agouti (*A^y*) mutation were generated by breeding R3 transgenic mice with KK-*A^y* strain mice. The obtained F1 littermates carrying the *A^y* mutation with or without a FLAG-Rheb transgene on C57BL/6 and a KK hybrid background (designated *A^y/Rheb* and *A^y*) were analyzed. This study was performed according to the guidelines of the animal ethics committee of Kobe University Graduate School of Medicine.

Islet preparation and immunoblot analysis. Islets were isolated by collagenase digestion followed by centrifugation over Histopaque medium (Sigma-Aldrich, St. Louis, MO). Cultured islets were extracted in buffer A (20 mmol/l Tris-HCl, pH 7.4, 120 mmol/l NaCl, 1 mmol/l EDTA, 5 mmol/l EGTA, 50 mmol/l β -glycerophosphate, 50 mmol/l NaF, 0.3% CHAPS, 1

mmol/l dithiothreitol, 4 μ g/ml leupeptin, and 4 μ g/ml aprotinin), and the supernatants were analyzed by immunoblotting with the indicated antibodies. The following antibodies were purchased from Cell Signaling Technologies (Beverly, MA): anti-phospho-S6 ribosomal protein (Ser235/236), anti-S6 ribosomal protein, anti-phospho-4EBP1 (Thr37/46), anti-phospho-4EBP1 (Thr70), anti-phospho-p70 S6 kinase (Thr389), anti-PKB, anti-phospho-PKB (Ser473), anti-phospho-p44/42 mitogen-activated protein (MAP) kinase (Thr202/Tyr204), and anti-p44/42 MAP kinase. Anti-IRS2 antibody was purchased from Upstate (Temecula, CA). Anti-Rheb antibody was kindly provided by N. Oshiro (Biosignal Research Center, Kobe University, Kobe, Japan).

Glucose tolerance testing and insulin tolerance testing. Mice were deprived of food for 16 h, and blood was collected from the tail vein after an oral injection (2 g/kg) or intraperitoneal injection (3 g/kg) of glucose. For insulin tolerance testing, mice fed ad libitum were injected with 0.75 units/kg body wt of human regular insulin.

Immunohistochemical and morphometric analysis of islets. Immunostaining for insulin and glucagon was performed using guinea pig antibodies against insulin and rabbit antibodies against glucagon (Dako Japan,

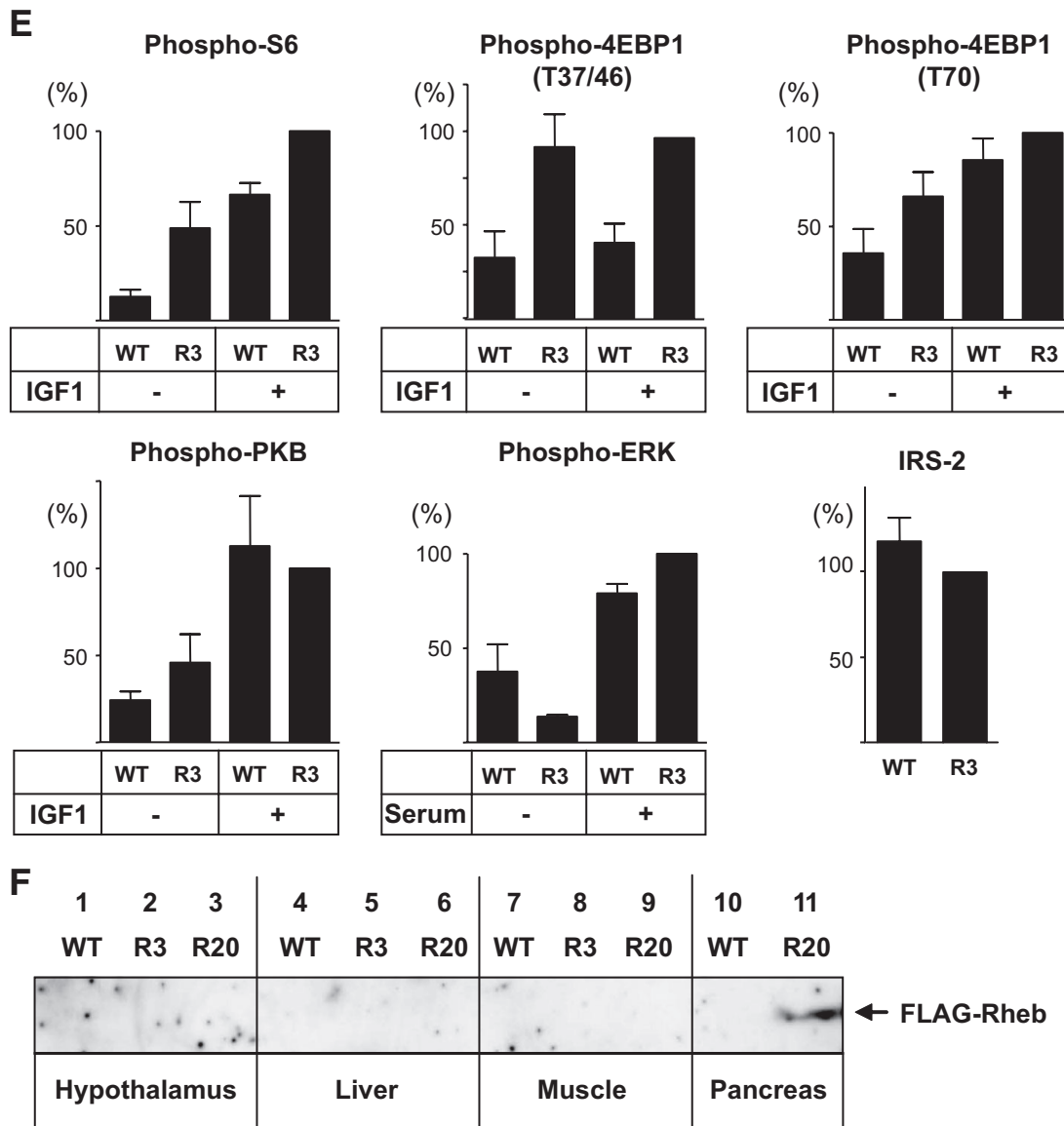


FIG. 1. Continued.

Kyoto, Japan). The immune complexes were detected with secondary antibodies conjugated with Cy3 or fluorescein isothiocyanate, respectively (Jackson ImmunoResearch Laboratories, West Grove, PA). For immunostaining of FLAG, phosphorylated S6, or Ki-67, after antigen retrieval by autoclave at 121°C for 15 min in 10 mmol/l sodium citrate (pH 6.0) and quenching of endogenous peroxidase with 3% H₂O₂ for 10 min, the sections were incubated with the anti-FLAG antibody (DYKDDDDK Tag antibody; Cell Signaling), anti-phospho-S6 ribosomal protein (Ser235/236), or anti-Ki-67 antibody (Dako Japan). Immunocomplexes were detected with a secondary antibody conjugated with horseradish peroxidase followed by incubation in diaminobenzidine peroxidase substrate solution. The immunostained sections were counterstained with hematoxylin. For quantification of β -cell and α -cell area, images of β - or α -cells and of the entire pancreas were obtained using a digital camera (BZ-8000; Keyence, Osaka, Japan) and analyzed using WinROOF software (Mitani, Fukui, Japan). The percentage of β - or α -cell area was calculated as the area of all insulin- or glucagon-positive cells based on the total pancreatic area surveyed. The β -cell mass was calculated by the percentage of β -cell area and pancreas weight. The relative β -cell size was calculated by dividing the β -cell area by the number of β -cell nuclei in the insulin-stained sections. Apoptotic β -cells were analyzed by immunostaining of insulin and terminal deoxynucleotidyl transferase dUTP nick-end labeling (TUNEL) assay using an ApopTag fluorescein in situ apoptosis detection kit (Chemicon International, Temecula, CA) according to the manufacturer's protocol.

Streptozotocin administration. Eight-week-old transgenic mice and wild-type littermates were injected intraperitoneally for 5 consecutive days with

streptozotocin (40 mg/kg or 50 mg/kg) dissolved just before injection in 0.1 mol/l citrate buffer.

Rapamycin administration. Mice were injected intraperitoneally with rapamycin (2 mg/kg) dissolved in 0.2% sodium carboxymethylcellulose and 0.25% Tween 80 or control vehicle three times a week from 5 to 8 weeks of age.

Statistical analysis. Data are expressed as the means \pm SE and were analyzed using the Mann-Whitney nonparametric *U* test. Two-tailed *P* values of <0.05 were considered statistically significant.

RESULTS

Expression of Rheb induces activation of the mTORC1 pathway in pancreatic β -cells. We confirmed the integration of the transgene in three independent founder lines (R3, R20, and R35; accession no. CDB0441T). Immunoblotting of total cellular extracts from pancreatic islets using the anti-Rheb antibody demonstrated that the transgene product was detected at a slightly higher level than endogenous Rheb on SDS-PAGE (Fig. 1A). Similar results were observed when FLAG-tagged Rheb was expressed transiently in HEK293 cells (data not shown), suggesting that the addition of a FLAG sequence to Rheb lowers the mobility of the polypeptide on SDS-PAGE. Immunoprecipitation with the anti-FLAG antibody fol-

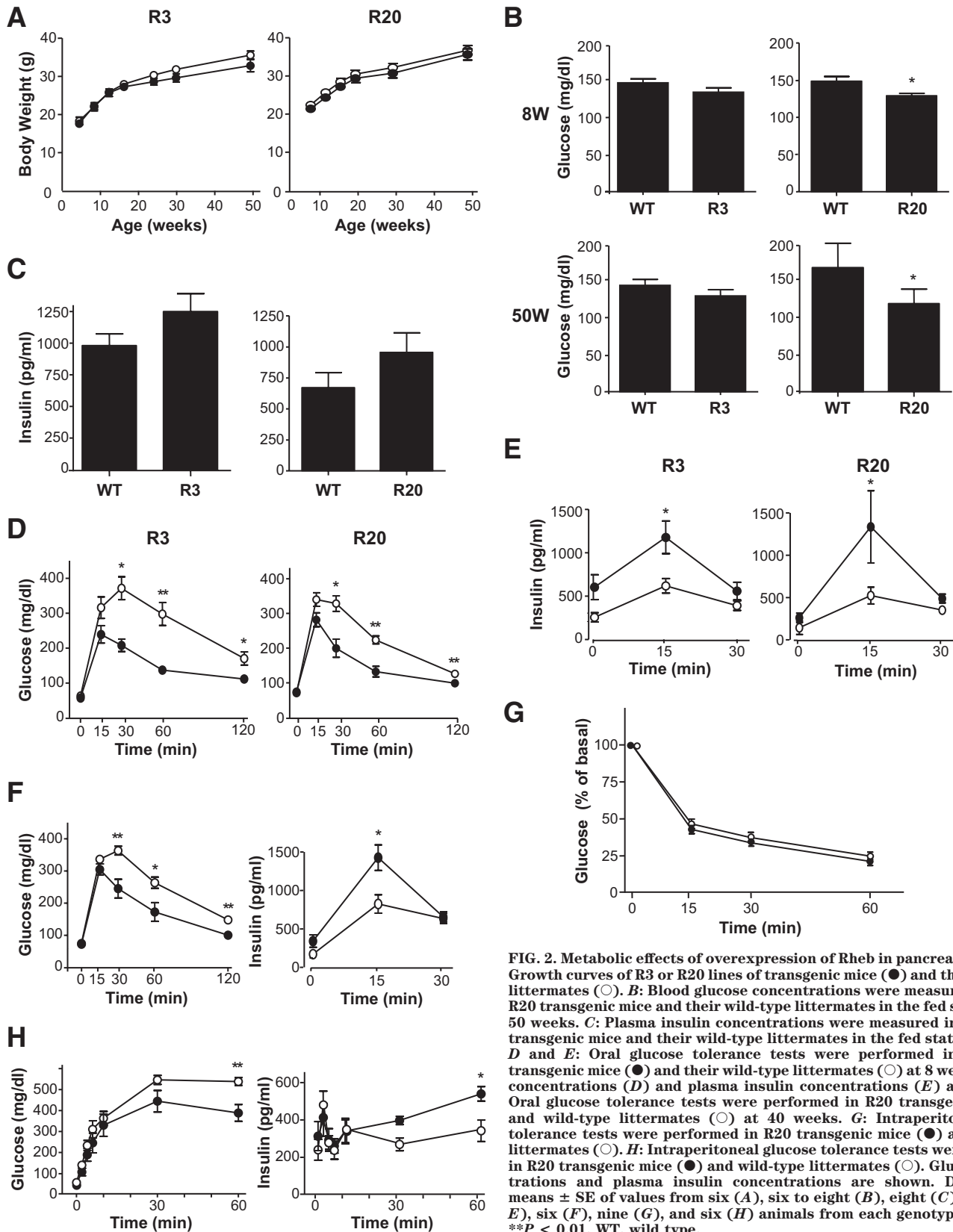


FIG. 2. Metabolic effects of overexpression of Rheb in pancreatic β -cells. **A:** Growth curves of R3 or R20 lines of transgenic mice (\bullet) and their wild-type littermates (\circ). **B:** Blood glucose concentrations were measured in R3 and R20 transgenic mice and their wild-type littermates in the fed state at 8 and 50 weeks. **C:** Plasma insulin concentrations were measured in R3 and R20 transgenic mice and their wild-type littermates in the fed state at 8 weeks. **D and E:** Oral glucose tolerance tests were performed in R3 or R20 transgenic mice (\bullet) and their wild-type littermates (\circ) at 8 weeks. Glucose concentrations (**D**) and plasma insulin concentrations (**E**) are shown. **F:** Oral glucose tolerance tests were performed in R20 transgenic mice (\bullet) and wild-type littermates (\circ) at 40 weeks. **G:** Intraperitoneal insulin tolerance tests were performed in R20 transgenic mice (\bullet) and wild-type littermates (\circ). **H:** Intraperitoneal glucose tolerance tests were performed in R20 transgenic mice (\bullet) and wild-type littermates (\circ). Glucose concentrations and plasma insulin concentrations are shown. Data are the means \pm SE of values from six (**A**), six to eight (**B**), eight (**C**), five (**D** and **E**), six (**F**), nine (**G**), and six (**H**) animals from each genotype. * $P < 0.05$; ** $P < 0.01$. WT, wild type.

lowed by immunoblotting with the same antibody failed to detect the expression of FLAG-Rheb in the hypothalamus, muscle, or liver, indicating that the expression of FLAG-Rheb is specific to the pancreatic β -cells (Fig. 1F).

To confirm the effect of the overexpression of Rheb in

β -cells, we examined the phosphorylation of the downstream effectors for mTORC1, ribosomal protein S6, and 4EBP1. Because the mTORC1 pathway is regulated in a nutrient-dependent manner, the ability of Rheb to activate the mTORC1 pathway is most easily visualized in nutrient-

TABLE 1
Metabolic characteristics of the transgenic mice and their wild-type littermates

	Plasma free fatty acids (mg/dl)	Plasma triglycerides (mg/dl)	Plasma leptin (ng/ml)
Wild type	1.46 ± 0.13	154.6 ± 9.4	2.09 ± 0.30
Transgenic	1.44 ± 0.77	166.8 ± 16.6	1.57 ± 0.21

Data are means ± SE of values from 7–10 animals from each genotype at 8 weeks for plasma triglycerides and leptin or at 10 weeks for plasma free fatty acids.

depleted conditions in vitro. Therefore, isolated islets were incubated for 2 h in 50% RPMI medium that was made by mixing RPMI with Krebs-Ringer bicarbonate buffer without FCS. Phosphorylation of S6 (Ser235/236) was clearly higher in islets prepared from transgenic mice than in those prepared from wild-type littermates (Fig. 1A). The immunoreactivity of the anti-phospho-S6 antibody appeared to parallel the abundance of FLAG-Rheb. The immunoreactivity of the anti-phospho-4EBP1 (Thr37/46) antibody increased in the islets prepared from transgenic mice in the same manner. When islets were stimulated with IGF-1, the immunoreactivities of the anti-phospho-S6 and anti-phospho-4EBP1 (Thr37/46 and Thr70) antibodies were increased in islets prepared from wild-type littermates, but the extent of immunoreactivity was still higher in islets from transgenic mice (Fig. 1B and E). The immunoreactivity of the anti-phospho-PKB (Ser473) was increased by IGF-1 stimulation in both wild-type and transgenic islets; however, the stimulation was greater in wild-type than in transgenic islets. The amount of IRS2 appeared to be relatively reduced in the transgenic islets compared with their wild-type littermates (Fig. 1C). This might be caused by a possible negative feedback mechanism induced by the activated p70 S6 kinase. Serum stimulation also induced phosphorylation of S6 and 4EBP1, but the stimulation was still greater in transgenic mice than in wild-type mice (Fig. 1D). Phosphorylation of MAPKs also increased after serum stimulation, but the stimulation was similar in both wild-type and transgenic islets. Subsequent studies were performed on animals derived from founder lines R3 and R20.

Improved glucose tolerance in transgenic mice. The rate of increase in body weight was not significantly different between the R3 and R20 lines of transgenic mice and their wild-type littermates (Fig. 2A). Metabolic parameters, including plasma triglycerides, free fatty acids, and leptin, were not significantly different between R3 transgenic mice and wild-type littermates either (Table 1). In contrast, R20 transgenic mice had significantly lower blood glucose concentrations in the fed state at 8 and 50 weeks compared with wild-type littermates (127.9 ± 4.24 vs. 145.6 ± 5.35 mg/dl at 8 weeks and 128.7 ± 6.16 vs. 147.9 ± 5.68 mg/dl at 50 weeks) (Fig. 2B). The plasma insulin levels in R20 mice were 1.43-fold those of wild-type littermates at 8 weeks (Fig. 2C). Although no significant differences in blood glucose concentrations were observed between R3 transgenic mice and wild-type littermates, the concentration tended to be lower in the transgenic mice, and this tendency was maintained to 50 weeks. Oral glucose tolerance testing at 8 weeks revealed that both the R3 and R20 lines of transgenic mice had improved glucose tolerance compared with wild-type littermates (Fig. 2D). Although fasting blood glucose con-

centrations were not significantly different between transgenic mice and wild-type littermates, both the R3 and R20 lines of transgenic mice had significantly lower blood glucose levels after glucose loading. Insulin release in response to glucose loading was significantly higher in transgenic mice than in wild-type littermates, with a 2.6-fold difference in R20 transgenic mice and a 1.7-fold difference in R3 transgenic mice at 15 min after injection (Fig. 2E). Similarly improved glucose tolerance was also observed at 40 weeks with the R20 transgenic mice (Fig. 2F). In contrast, both R20 (Fig. 2G) and R3 transgenic mice (data not shown) demonstrated similar insulin responsiveness after intraperitoneal injections of insulin. Then, intraperitoneal glucose tolerance testing was performed to measure the in vivo glucose-stimulated insulin secretion in the early and late phases (Fig. 2H). Although glucose concentration did not differ significantly between transgenic mice and wild-type littermates in the early phase, the glucose concentration was significantly lower in the transgenic mice in the late phase. Insulin secretion was similar in transgenic mice and their wild-type littermates in the early phase, but it was significantly higher in transgenic mice than in their wild-type littermates in the late phase. Taken together, these results indicate that the improved glucose tolerance in the transgenic mice can be attributable mainly to a greater ability to secrete insulin in the late phase.

Increased β -cell mass and cell growth in transgenic mice. Hematoxylin and eosin staining of the sections revealed that the pancreatic islet architecture was grossly unchanged in mice from ages 8 to 90 weeks (Fig. 3A and D). Immunostaining of the sections with the anti-FLAG antibody confirmed the expression of FLAG-Rheb in the islets of transgenic mice from ages 8 to 90 weeks (Fig. 3B and D). Immunostaining with the anti-phospho-S6 antibody appeared lower in the islet areas than in the exocrine acinar areas. However, the dark-staining cells in the islets appeared more abundant in transgenic mice than in the wild-type littermates (Fig. 3C). The ratio of the number of the dark staining cells to the number of nuclei in the islets was significantly higher in transgenic mice than in wild-type littermates (19.48 ± 3.23 vs. 6.76 ± 1.14%).

Immunostaining with the anti-insulin and anti-glucagon antibodies also demonstrated the grossly unchanged structures of pancreatic islets (Fig. 3E). Quantitative determination of β -cell area relative to pancreatic area in insulin-stained sections revealed that the β -cell area was significantly higher (1.46-fold) in R3 transgenic mice than in wild-type littermates (0.581 ± 0.048 vs. 0.399 ± 0.040%) (Fig. 3F). In contrast, the α -cell area did not differ significantly between the R3 transgenic and wild-type littermates (0.144 ± 0.028 vs. 0.134 ± 0.018%). β -Cell mass was also significantly increased in R3 transgenic mice compared with wild-type littermates (1,070 ± 63.6 vs. 712.5 ± 60.9 μ g) (Fig. 3G). The relative β -cell size was significantly increased at 1.30-fold in the transgenic mice compared with wild-type littermates (253.7 ± 14.56 vs. 197.6 ± 5.0 μ m²) (Fig. 3H). To evaluate the involvement of β -cell proliferation in the increase of β -cell mass in the transgenic mice, immunostaining with the anti-Ki-67 antibody was performed (Fig. 3I). As shown in Table 2, we did not observe significant differences in the proportion of Ki-67-positive nuclei in the islets between wild-type and transgenic mice. To evaluate the involvement of apoptotic β -cells, TUNEL assay was performed but could not detect significant amounts of apoptotic cells at the basal state.

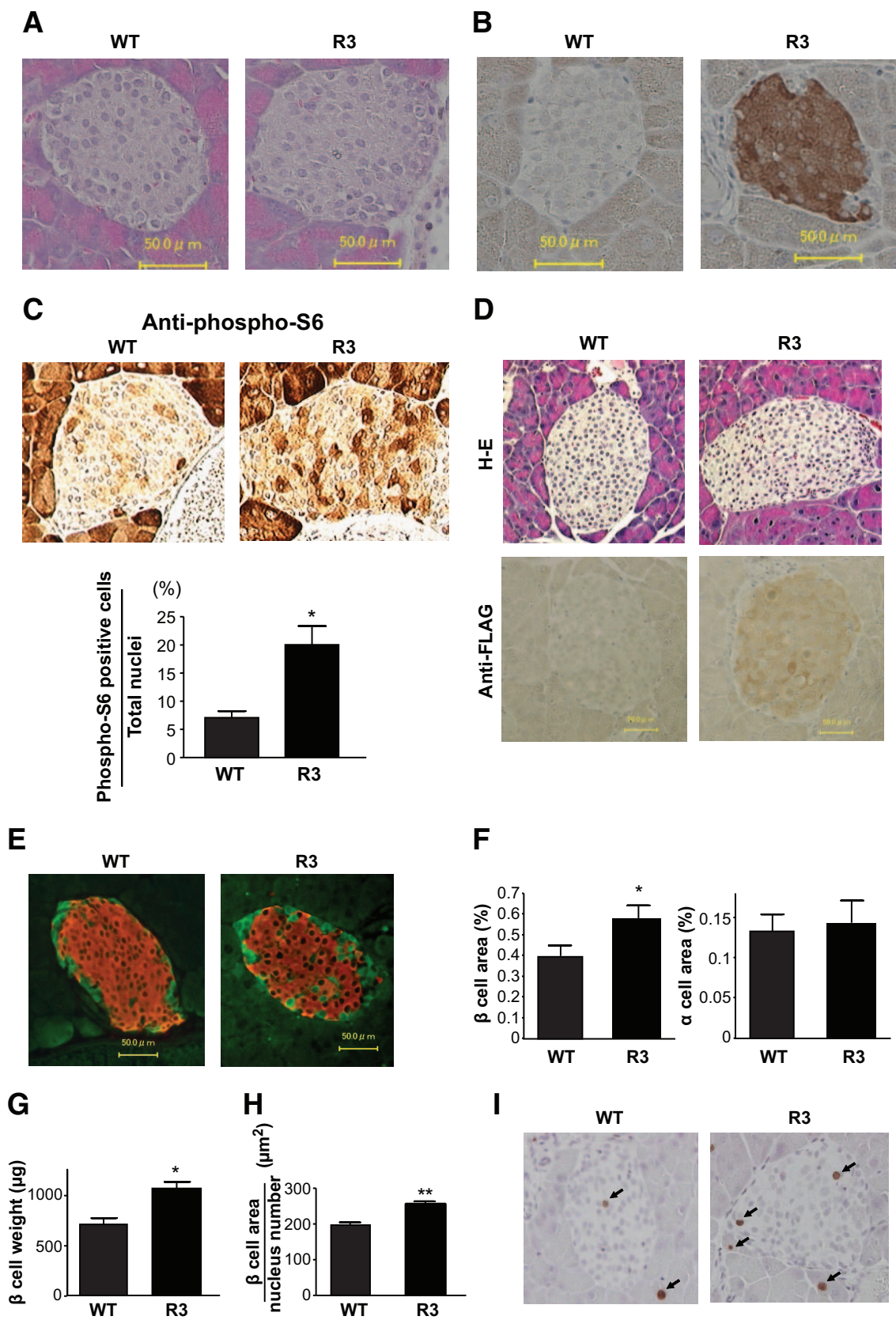


FIG. 3. Increased β -cell mass and cell growth in transgenic mice. **A:** Hematoxylin and eosin staining of representative pancreatic sections from 8-week-old R3 transgenic mice and their wild-type littermates. **B** and **C:** Immunostaining with the anti-FLAG antibody (**B**) and anti-phospho-S6 (Ser235/236) antibody (**C**, upper panels) of representative pancreatic sections from 8-week-old R3 transgenic mice and wild-type littermates. Ratio of the number of dark staining cells to the total number of nuclei in islets from transgenic mice and wild-type littermates is shown (**C**, lower panels). **D:** Hematoxylin and eosin (H-E) staining and immunostaining with the anti-FLAG antibody of representative pancreatic sections from 90-week-old R3 transgenic mice and their wild-type littermates. **E:** Immunostaining with the anti-insulin (red) and the anti-glucagon (green) antibodies of representative pancreatic sections from 8-week-old R3 transgenic mice and their wild-type littermates. **F:** Quantification of β - and

TABLE 2
Numbers of total and Ki-67–positive nuclei in islets

	Counted islets per animal	Counted nuclei per animal	Nuclei per islet	Proportion of Ki-67–positive nuclei per islet (%)
Wild type	68	6,297 ± 664.5	93 ± 7.6	1.10 ± 0.08
Transgenic	60	5,291 ± 567.7	89 ± 9.7	1.16 ± 0.13

Data are means ± SE of values from four animals from each genotype. Pancreatic sections were immunostained with the anti-Ki-67 antibody followed by counterstaining with hematoxylin as shown in Fig. 3I. Numbers of all nuclei and of Ki-67–positive nuclei in the islets of wild-type and transgenic mice were counted.

Prevention of streptozotocin- and obesity-induced hyperglycemia in transgenic mice. To determine whether Rheb overexpression in pancreatic β -cells prevented hyperglycemia in pathophysiological conditions, we used two models of experimentally induced diabetes: streptozotocin-induced and obesity-induced. First, R3 line transgenic mice and wild-type littermates were subjected to intraperitoneal injections of streptozotocin at 40 or 50 mg/kg for 5 consecutive days. Monitoring of blood glucose levels in the fed state revealed that wild-type littermates had significant hyperglycemia by 1 or 3 weeks after starting injections at doses of 50 or 40 mg/kg, respectively. By contrast, R3 transgenic mice remained resistant to hyperglycemia (175.5 ± 13.5 vs. 135.3 ± 8.87 mg/dl at 40 mg/kg, and 327.0 ± 2.27 vs. 156.8 ± 7.52 mg/dl at 50 mg/kg 4 weeks after injection) (Fig. 4A). R20 line transgenic mice also exhibited the same resistance to hyperglycemia induced by streptozotocin as the R3 transgenic mice (Fig. 4B). The insulin level of the wild-type and transgenic mice decreased to 25.3 and 33.4%, respectively, of the levels in the nontreated wild-type and transgenic mice of the same age (Fig. 4C). However, the glucose-to-insulin ratio differed significantly between transgenic mice and their wild-type littermates 4 weeks after injection ($4.79 \pm 0.51 \times 10^6$ wt/wt vs. $16.34 \pm 4.93 \times 10^6$ wt/wt) (Fig. 4D). Because the insulin sensitivity did not differ between wild-type and transgenic mice, as described above, the significant difference in the glucose-to-insulin ratios suggests that the amount of insulin secreted in response to blood glucose concentration differed between groups. Oral glucose tolerance testing demonstrated clearly that transgenic mice were able to secrete more insulin than wild-type littermates in response to glucose loading (Fig. 4E), although the maximum production of insulin was reduced even in transgenic mice when compared with the results shown in Fig. 2E. Consistent with the decrease in the serum insulin levels, immunohistological analysis demonstrated that β -cell areas were decreased in both transgenic mice and wild-type littermates compared with nontreated mice. However, the β -cell area was significantly higher in transgenic mice than in wild-type littermates (0.340 ± 0.025 vs. $0.243 \pm 0.030\%$) (Fig. 4F and G). TUNEL staining of the pancreatic sections showed no significant difference in the extent of apoptosis in β -cells 1 week after administration with streptozotocin (Fig. 4H and Table 3).

TABLE 3
Numbers of insulin- and TUNEL-positive nuclei in islets

	Counted islets per animal	Counted nuclei per animal	Nuclei per islet	Proportion of TUNEL-positive nuclei per islet (%)
Wild type	69	2,882 ± 567.8	43 ± 4.3	0.55 ± 0.15
Transgenic	65	3,233 ± 495.5	46 ± 4.0	0.42 ± 0.11

Data are means ± SE of values from five animals from each genotype. Pancreatic sections were double-stained with the anti-insulin antibody and TUNEL assay 1 week after 50 mg/kg streptozotocin administration as shown in Fig. 4H. Numbers of all nuclei and of TUNEL-positive nuclei in the insulin-positive cells of wild-type and transgenic mice were counted.

Second, as a model of obesity-induced diabetes, we generated R3 transgenic mice with the lethal yellow agouti (A^y) mutation by breeding R3 transgenic mice with $KK-A^y$ mice. For analysis we used F1 offspring littermates carrying the A^y mutation with or without a FLAG-Rheb transgene on a C57BL/6 and KK mouse strain hybrid background (designated $A^y/Rheb$ and A^y , respectively). The rate of increase in body weight was not significantly different between $A^y/Rheb$ and A^y mice (35.5 ± 0.94 vs. 37.5 ± 1.06 g at 10 weeks). Oral glucose tolerance testing revealed that the $A^y/Rheb$ mice had improved glucose tolerance (Fig. 5A). Although blood glucose concentrations in the fasting state were not significantly different between $A^y/Rheb$ and A^y mice, the $A^y/Rheb$ mice had significantly lower blood glucose levels at 60 and 120 min after glucose loading. Thus, the glucose concentration in A^y mice remained at 424 ± 39.8 mg/dl at 60 min and 363.4 ± 47.9 mg/dl at 120 min, whereas that in $A^y/Rheb$ mice was 210 ± 46.6 mg/dl at 60 min and returned to 116.2 ± 17.91 mg/dl at 120 min. The improved glucose tolerance in $A^y/Rheb$ mice was attributable to higher insulin release, with a significant 2.2-fold level at 15 min and a 1.9-fold level at 30 min after glucose loading compared with A^y mice.

Elimination of the effect of Rheb expression by the administration with rapamycin. To examine whether the phenotypes observed above are dependent on the mTORC1 pathway, mice were injected intraperitoneally with mTORC1 inhibitor rapamycin from 5 to 8 weeks of age, and glucose tolerance testing was performed at 8 weeks (Fig. 5B). At 15, 30, 60, and 120 min after glucose loading, blood glucose concentration was ~ 50 mg/dl higher in rapamycin-treated mice than in untreated mice. Notably, glucose tolerance was similar in rapamycin-treated transgenic mice and in rapamycin-treated wild-type littermates. In addition, the improved insulin secretion in transgenic mice was eliminated completely to the level observed in their wild-type littermates. Immunoblot analysis of the islets prepared from rapamycin- or vehicle-treated mice demonstrated that phosphorylation of S6 and 4EBP1 were reduced by rapamycin administration in both transgenic mice and wild-type littermates, indicating that the effect of rapamycin was achieved by suppression of mTORC1 activity (Fig. 5C).

α -cell area as a percentage of total pancreatic area in transgenic mice and their wild-type littermates. G: β -Cell mass was calculated by the β -cell area and pancreas weight. H: The relative size of β -cells in the transgenic mice and their wild-type littermates was calculated. I: Immunostaining with anti-Ki-67 antibody of representative pancreatic sections from 9-week-old R3 transgenic mice and their wild-type littermates. Data are the means ± SE of values from four (C), five (F), four (G), and five (H) animals from each genotype. * $P < 0.05$; ** $P < 0.01$. WT, wild type. (A high-quality digital representation of this figure is available in the online issue.)

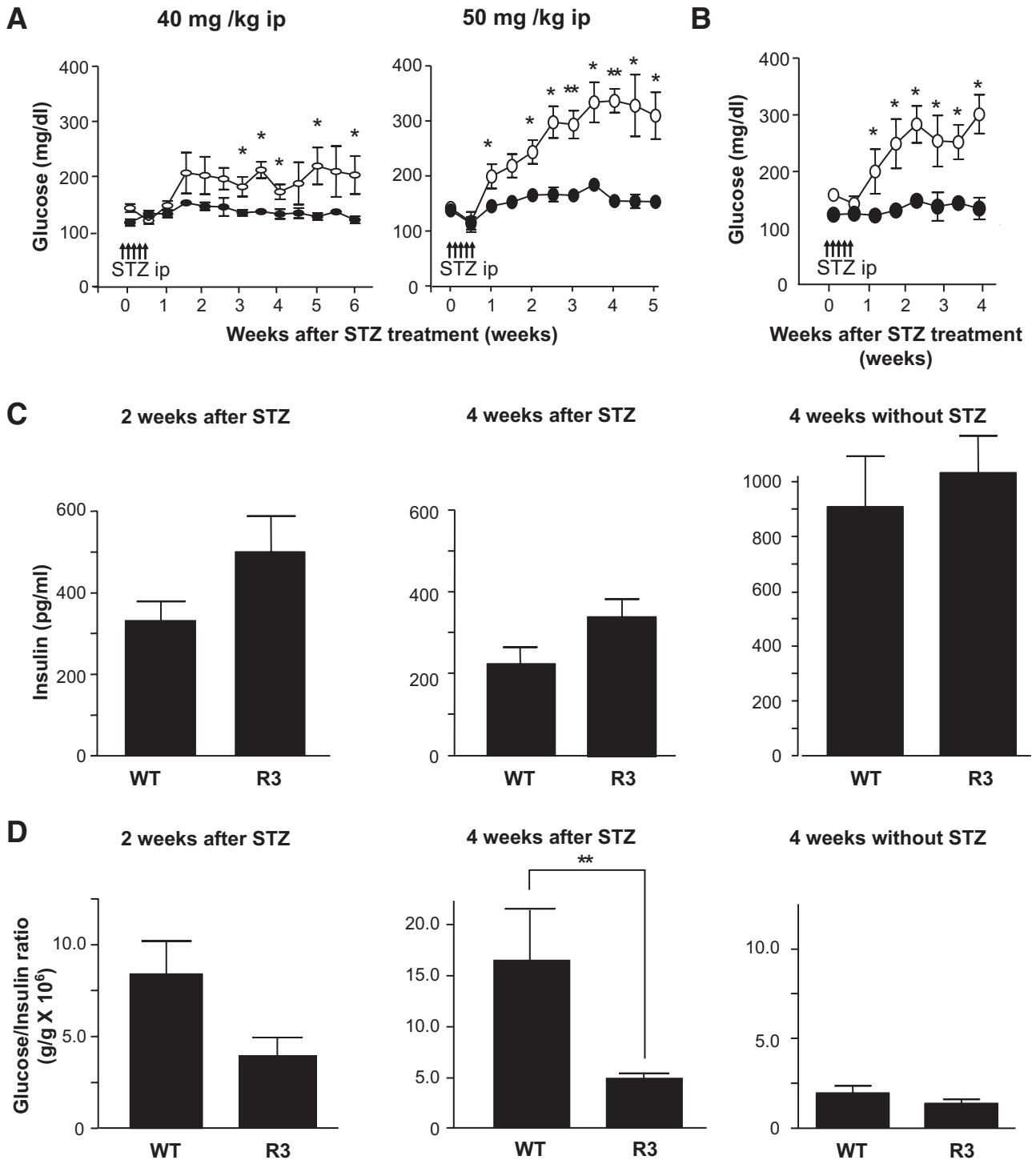


FIG. 4. Transgenic mice were resistant to streptozotocin-induced hyperglycemia. **A:** Doses of 40 mg/kg or 50 mg/kg streptozotocin were administered to R3 line transgenic mice (●) or wild-type littermates (○) for 5 consecutive days (arrows in the figure). Blood glucose concentrations in the fed state were monitored. Data are the means \pm SE of values from four (40 mg/kg) or five (50 mg/kg) animals from each genotype. **B:** A dose of 50 mg/kg streptozotocin was administered to R20 transgenic mice (●) or wild-type littermates (○), and blood glucose concentrations were monitored with mice in the fed state. Data are the means \pm SE of values from four animals from each genotype. **C and D:** Plasma insulin concentration (**C**) and glucose-to-insulin ratio (**D**) after administration with or without 50 mg/kg streptozotocin as shown in **A**. **E:** Oral glucose tolerance tests were performed in R20 transgenic mice (●) and wild-type littermates (○) 4 weeks after streptozotocin administration as shown in **B**. Glucose and insulin concentrations are shown. **F:** Immunostaining with the anti-insulin (red) and anti-glucagon (green) antibodies of representative pancreatic sections from R3 transgenic mice (R3) and their wild-type littermates (WT) 4 weeks after 50 mg/kg streptozotocin administration as shown in **A**. **G:** Quantification of β -cell area as a percentage of total pancreatic area in transgenic mice and their wild-type littermates 4 weeks after administration with or without 50 mg/kg streptozotocin as shown in **A**. **H:** Immunostaining with anti-insulin (red) antibody and TUNEL assay (green) of representative pancreatic sections from the transgenic mice and their wild-type littermates 1 week after 50 mg/kg streptozotocin administration. Values represent the means \pm SE. * $P < 0.05$; ** $P < 0.01$. (A high-quality digital representation of this figure is available in the online issue.)

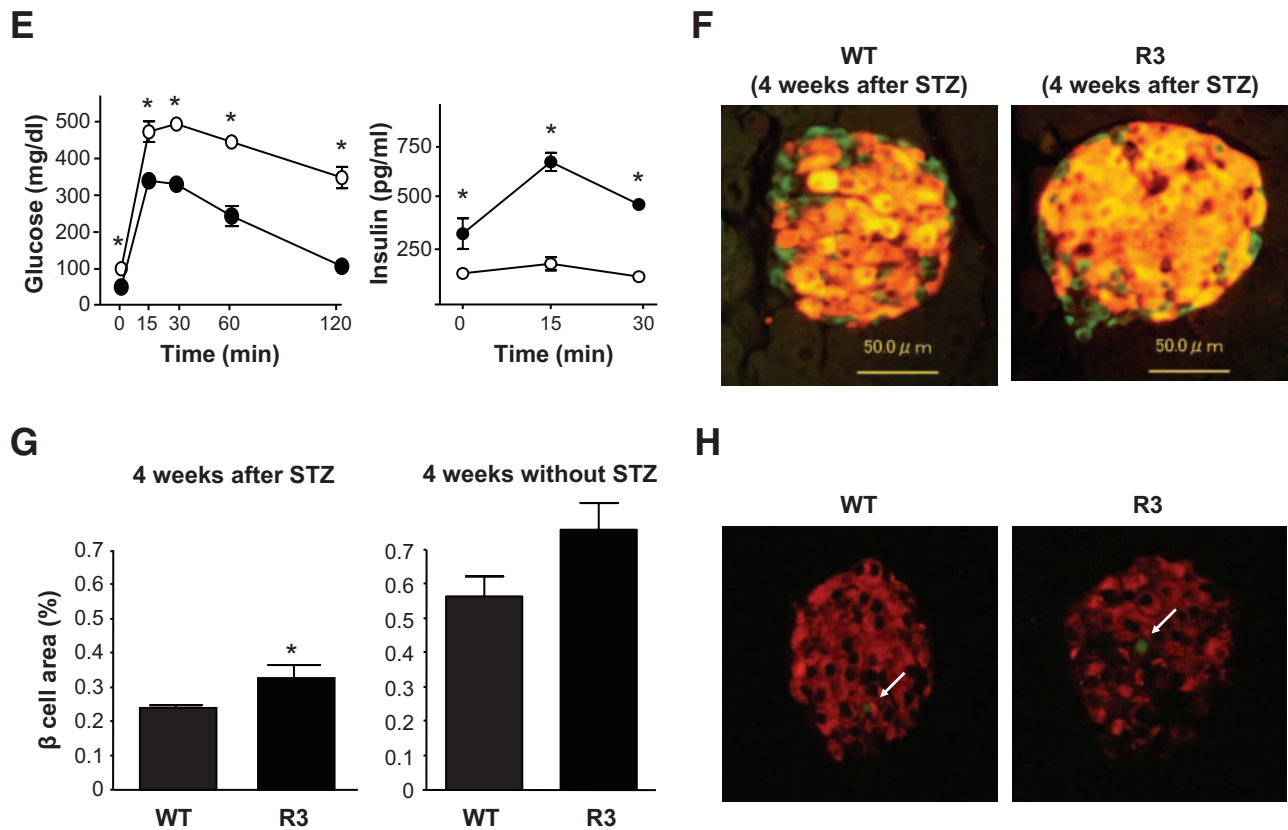


FIG. 4. Continued.

DISCUSSION

To examine the role of the mTORC1 pathway in pancreatic β -cells in vivo, we produced transgenic mice that express Rheb under the control of the rat insulin promoter. Rheb is unique in that it maintains basal levels of GTP charging much higher than those of Ras because of its lower intrinsic GTPase activity. With a limiting level of endogenous Rheb GTPase-activating activity established by the TSC complex, even wild-type Rheb takes an active GTP form when it is overexpressed (21). When isolated islets were incubated in nutrient-limited media, phosphorylation levels of ribosomal protein S6 and of 4EBP1 were clearly augmented in transgenic β -cells compared with wild-type β -cells, in parallel with the abundance of FLAG-Rheb. Moreover, immunostaining of the pancreas sections with the anti-phospho-S6 antibody revealed an increase in S6 phosphorylation in the transgenic β -cells. These results indicate that the mTORC1 pathway is upregulated in the pancreatic β -cells of transgenic mice in vivo as well as in vitro.

We found that these transgenic mice had improved glucose tolerance because of a higher capacity to secrete insulin in response to glucose loading. We also found that the increase in insulin secretion was mediated mainly by the increased secretion in the late phase. Morphometry proved that the increase in the capacity to produce insulin could be attributed to an increase in the β -cell mass, which was accompanied by increased β -cell size. These results are consistent with previous reports that overexpression of Rheb as well as loss-of-function mutations of the genes encoding TSC1 or TSC2 results in enlarged cell size (23–28,36).

Overexpression of Rheb might induce dysfunction of

β -cells because inappropriate activation of the TSC/Rheb pathway leads to the downregulation of the insulin/IGF-1 signaling system as a result of degradation of IRS1 and -2 (37–41). Moreover, constitutive activation of the mTOR pathway by loss of the *TSC1* or *TSC2* genes in cell lines and tumors causes endoplasmic reticulum stress, resulting in inhibition of insulin action and an increase in vulnerability to apoptosis (42). Consistent with these reports, Shigeyama et al. (43) demonstrated that mice deficient in *TSC2* in pancreatic β -cells developed progressive hyperglycemia after 40 weeks of age, although the mice also exhibited hypoglycemia and hyperinsulinemia when young, suggesting that downregulation of insulin action or endoplasmic reticulum stress might occur with aging. By contrast, transgenic mice tended to have lower glucose levels and improved glucose tolerance even at 40–50 weeks. The histological analysis of islets of even 90-week-old mice confirmed no adverse effect on pancreatic β -cells. Although the IRS2 level appeared to be relatively reduced in transgenic islets, the extent of the mTORC1 activation might not be strong enough to induce adverse effects on the β -cells in these transgenic mice.

Upregulation of IRS2 and Akt or deletion of *Pten* induces an increase in β -cell mass and resistance to hyperglycemia (6,7,44). A similar phenotype has been reported for the downregulation of more distal negative mediators of Akt, FoxO1, and p27^{kip1} (15,16,45). These phenotypes are mediated by increased proliferation of β -cells as well as an increase in β -cell size. Reciprocally, mice deficient for p70S6K or knock-in mice whose S6 protein contains alanine substitutions at all five phosphorylatable serine residues show reduced insulin secretion in response to glucose caused by diminished β -cell size (5,17). Because

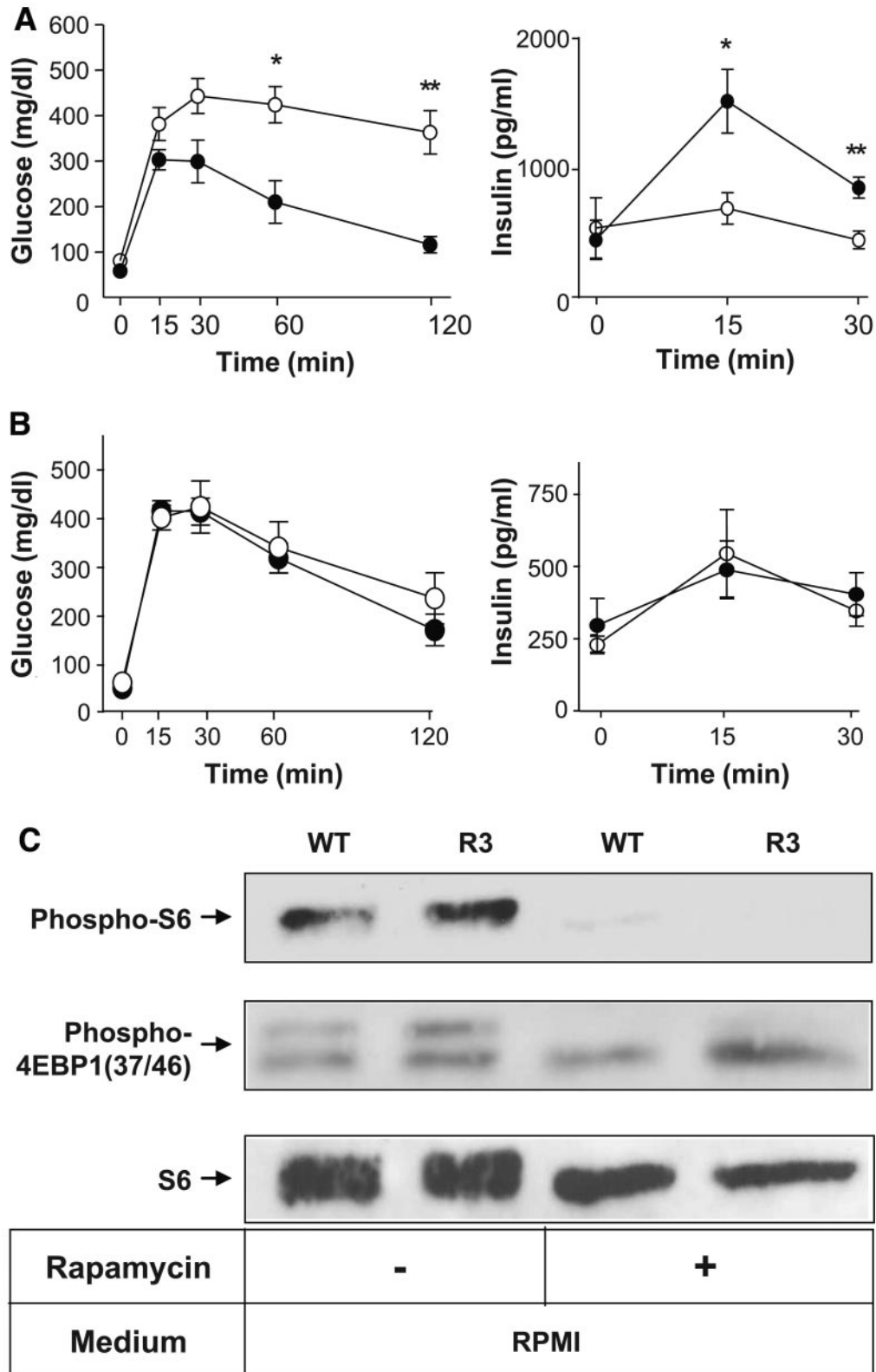


FIG. 5. *A*: Transgenic mice were resistant to obesity-induced hyperglycemia. Oral glucose tolerance tests were performed in A^y/Rheb mice (●) and A^y littermates (○). Blood glucose concentrations and plasma insulin concentrations are shown. *B*: Elimination of the effect of Rheb expression in β -cells after administration with rapamycin. Oral glucose tolerance tests were performed in rapamycin-treated transgenic mice (●) and their rapamycin-treated wild-type littermates (○). Blood glucose and plasma insulin concentrations are shown. Data are the means \pm SE of values from five (*A* and *B*) animals from each genotype. *C*: Islets were prepared from rapamycin- or vehicle-treated mice of each genotype and incubated for 1 h in RPMI, and the same amounts of cellular extracts were analyzed by immunoblotting with the antibodies to phospho-S6 ribosomal protein (Ser235/236), phospho-4EBP1 (Thr37/46), or S6 ribosomal protein. **P* < 0.05; ***P* < 0.01. WT, wild type.

Rheb has been reported to be required for both cell cycle progression and cell growth in *Drosophila* (28), and because mTORC1 is involved in cell proliferation in some mammalian cells such as cancer cells, it might be premature to conclude only from Ki-67 staining that cell proliferation is not involved in our mouse model.

It should be noted that transgenic mice exhibited resistance to hyperglycemia induced by low-dose streptozotocin as well as by obesity. Although streptozotocin administration induced a reduction of β -cell areas by ~43–45% in both wild-type and transgenic mice, insulin secretion in response to glucose loading was much higher in transgenic mice than in wild-type littermates. This suggests that the residual β -cell function in transgenic mice might be higher than that in wild-type littermates.

We cannot exclude completely the possibility that overexpression of Rheb might affect intracellular signals other than mTORC1 pathways. Rheb has been reported to inhibit the Raf-dependent MAPK pathway through the interaction of the Ras-binding domain of B-Raf or cRaf in a rapamycin-insensitive manner (46–48). However, serum stimulation of MAPK phosphorylation did not appear to decrease in the transgenic islets compared with their wild-type littermates. In addition, rapamycin administration eliminated the improved insulin secretion in the transgenic mice completely to the level observed in wild-type littermates. Given that MAPKs are not affected significantly by rapamycin, these results suggest that the rapamycin-sensitive mTORC1 pathway plays a crucial role in this mouse model.

In conclusion, our findings highlight the importance of the role of the mTORC1 pathway in pancreatic β -cells. Activation of the mTORC1 pathway by Rheb led to an increase in β -cell mass and protection from hyperglycemia induced by β -cell injury and by insulin resistance. Further elucidation of the intracellular signaling mediated by Rheb in pancreatic β -cells might thus provide a basis for the development of new therapeutic strategies to improve insulin secretion and thereby prevent the development of diabetes.

ACKNOWLEDGMENTS

This work was supported by a grant for the 21st Century COE Program “Center of Excellence for Signal Transduction Disease: Diabetes Mellitus as a Model” and research grants from the Ministry of Education, Culture, Sports, Science and Technology of Japan (to K.H.).

No potential conflicts of interest relevant to this article were reported.

Parts of this study were presented in abstract form at the 68th American Diabetes Association Scientific Sessions, San Francisco, California, 6–10 June 2008.

We thank Domenico Accili for the generous gift of rat insulin promoter plasmid and Noriko Oshiro for the generous gift of anti-Rheb antibody and Rheb cDNA. We thank Atsumi Katsuta for her technical assistance. We are grateful to Ushio Kikkawa for helpful discussion and continuous support.

REFERENCES

- Kasuga M. Insulin resistance and pancreatic β -cell failure. *J Clin Invest* 2006;116:1756–1760
- Rhodes CJ. Type 2 diabetes: a matter of β -cell life and death? *Science* 2005;307:380–384
- Withers DJ, Gutierrez JS, Towery H, Burks DJ, Ren JM, Previs S, Zhang Y, Bernal D, Pons S, Shulman GI, Bonner-Weir S, White MF. Disruption of IRS-2 causes type 2 diabetes in mice. *Nature* 1998;391:900–904
- Kulkarni RN, Bruning JC, Winnay JN, Postic C, Magnuson MA, Kahn CR. Tissue-specific knockout of the insulin receptor in pancreatic β -cells creates an insulin secretory defect similar to that in type 2 diabetes. *Cell* 1999;96:329–339
- Pende M, Kozma SC, Jaquet M, Oorschot V, Burcelin R, Le Marchand-Brustel Y, Klumperman J, Thorens B, Thomas G. Hypoinsulinaemia, glucose intolerance and diminished β -cell size in S6K1-deficient mice. *Nature* 2000;408:994–997
- Tuttle RL, Gill NS, Pugh W, Lee JP, Koeberlein B, Furth EE, Polonsky KS, Naji A, Birnbaum MJ. Regulation of pancreatic β -cell growth and survival by the serine/threonine protein kinase Akt1/PKB α . *Nat Med* 2001;7:1133–1137
- Bernal-Mizrachi E, Wen W, Stahlhut S, Welling CM, Permutt MA. Islet β -cell expression of constitutively active Akt1/PKB α induces striking hypertrophy, hyperplasia, and hyperinsulinemia. *J Clin Invest* 2001;108:1631–1638
- Hashimoto N, Kido Y, Uchida T, Matsuda T, Suzuki K, Inoue H, Matsumoto M, Ogawa W, Maeda S, Fujihara H, Ueta Y, Uchiyama Y, Akimoto K, Ohno S, Noda T, Kasuga M. PKC λ regulates glucose-induced insulin secretion through modulation of gene expression in pancreatic β -cells. *J Clin Invest* 2005;115:138–145
- Stiles BL, Kuralwalla-Martinez C, Guo W, Gregorian C, Wang Y, Tian J, Magnuson MA, Wu H. Selective deletion of *Pten* in pancreatic β -cells leads to increased islet mass and resistance to STZ-induced diabetes. *Mol Cell Biol* 2006;26:2772–2781
- Hashimoto N, Kido Y, Uchida T, Asahara S, Shigeyama Y, Matsuda T, Takeda A, Tsuchihashi D, Nishizawa A, Ogawa W, Fujimoto Y, Okamura H, Arden KC, Herrera PL, Noda T, Kasuga M. Ablation of PDK1 in pancreatic β -cells induces diabetes as a result of loss of β -cell mass. *Nat Genet* 2006;38:589–593
- Ueki K, Okada T, Hu J, Liew CW, Assmann A, Dahlgren GM, Peters JL, Shackman JG, Zhang M, Artner I, Satin LS, Stein R, Holzenberger M, Kennedy RT, Kahn CR, Kulkarni RN. Total insulin and IGF-I resistance in pancreatic β -cells causes overt diabetes. *Nat Genet* 2006;38:583–588
- Wullschlegel S, Loewith R, Hall MN. TOR signaling in growth and metabolism. *Cell* 2006;124:471–484
- Sarbassov DD, Ali SM, Sabatini DM. Growing roles for the mTOR pathway. *Curr Opin Cell Biol* 2005;17:596–603
- Isotani S, Hara K, Tokunaga C, Inoue H, Avruch J, Yonezawa K. Immunopurified mammalian target of rapamycin phosphorylates and activates p70 S6 kinase α in vitro. *J Biol Chem* 1999;274:34493–34498
- Nakae J, Biggs WH III, Kitamura T, Cavenee WK, Wright CV, Arden KC, Accili D. Regulation of insulin action and pancreatic β -cell function by mutated alleles of the gene encoding forkhead transcription factor Foxo1. *Nat Genet* 2002;32:245–253
- Kitamura T, Nakae J, Kitamura Y, Kido Y, Biggs WH III, Wright CV, White MF, Arden KC, Accili D. The forkhead transcription factor Foxo1 links insulin signaling to *Pdx1* regulation of pancreatic β -cell growth. *J Clin Invest* 2002;110:1839–1847
- Ruvinsky I, Sharon N, Lerer T, Cohen H, Stolovich-Rain M, Nir T, Dor Y, Zisman P, Meyuhas O. Ribosomal protein S6 phosphorylation is a determinant of cell size and glucose homeostasis. *Genes Dev* 2005;19:2199–2211
- Hara K, Maruki Y, Long X, Yoshino K, Oshiro N, Hidayat S, Tokunaga C, Avruch J, Yonezawa K. Raptor, a binding partner of target of rapamycin (TOR), mediates TOR action. *Cell* 2002;110:177–189
- Kim DH, Sarbassov DD, Ali SM, Latek RR, Guntur KV, Erdjument-Bromage H, Tempst P, Sabatini DM. GbetaL, a positive regulator of the rapamycin-sensitive pathway required for the nutrient-sensitive interaction between raptor and mTOR. *Mol Cell* 2003;11:895–904
- Aspuria PJ, Tamanoi F. The Rheb family of GTP-binding proteins. *Cell Signal* 2004;16:1105–1112
- Avruch J, Hara K, Lin Y, Liu M, Long X, Ortiz-Vega S, Yonezawa K. Insulin and amino-acid regulation of mTOR signaling and kinase activity through the Rheb GTPase. *Oncogene* 2006;25:6361–6372
- Long X, Lin Y, Ortiz-Vega S, Yonezawa K, Avruch J. Rheb binds and regulates the mTOR kinase. *Curr Biol* 2005;15:702–713
- Tapon N, Ito N, Dickson BJ, Treisman JE, Hariharan IK. The *Drosophila* tuberous sclerosis complex gene homologs restrict cell growth and cell proliferation. *Cell* 2001;105:345–355
- Potter CJ, Huang H, Xu T. *Drosophila* Tsc1 functions with Tsc2 to antagonize insulin signaling in regulating cell growth, cell proliferation, and organ size. *Cell* 2001;105:357–368
- Gao X, Pan D. TSC1 and TSC2 tumor suppressors antagonize insulin signaling in cell growth. *Genes Dev* 2001;15:1383–1392
- Stocker H, Radimerski T, Schindelholt B, Wittwer F, Belawat P, Daram P,

- Breuer S, Thomas G, Hafen E. Rheb is an essential regulator of S6K in controlling cell growth in *Drosophila*. *Nat Cell Biol* 2003;5:559–565
27. Saucedo LJ, Gao X, Chiarelli DA, Li L, Pan D, Edgar BA. Rheb promotes cell growth as a component of the insulin/TOR signaling network. *Nat Cell Biol* 2003;5:566–571
28. Patel PH, Thapar N, Guo L, Martinez M, Maris J, Gau CL, Lengyel JA, Tamanoi F. *Drosophila* Rheb GTPase is required for cell cycle progression and cell growth. *J Cell Sci* 2003;116:3601–3610
29. Garami A, Zwartkruis FJT, Nobukuni T, Joaquin M, Rocco M, Stocker H, Kozma SC, Hafen E, Bos JL, Thomas G. Insulin activation of Rheb, a mediator of mTOR/S6K/4E-BP signaling, is inhibited by TSC1 and 2. *Mol Cell* 2003;11:1457–1466
30. Tee AR, Manning BD, Roux PP, Cantley LC, Blenis J. Tuberous sclerosis complex gene products, Tuberin and Hamartin, control mTOR signaling by acting as a GTPase-activating protein complex toward Rheb. *Curr Biol* 2003;13:1259–1268
31. Gao X, Zhang Y, Arrazola P, Hino O, Kobayashi T, Yeung RS, Ru B, Pan D. Tsc tumour suppressor proteins antagonize amino-acid-TOR signaling. *Nat Cell Biol* 2002;4:699–704
32. Hara K, Yonezawa K, Weng QP, Kozlowski MT, Belham C, Avruch J. Amino acid sufficiency and mTOR regulate p70 S6 kinase and eIF-4E BP1 through a common effector mechanism. *J Biol Chem* 1998;273:14484–14494
33. Long X, Ortiz-Vega S, Lin Y, Avruch J. Rheb binding to mammalian target of rapamycin (mTOR) is regulated by amino acid sufficiency. *J Biol Chem* 2005;280:23433–23436
34. Inoki K, Zhu T, Guan KL. TSC2 mediates cellular energy response to control cell growth and survival. *Cell* 2003;115:577–590
35. Bai X, Ma D, Liu A, Shen X, Wang QJ, Liu Y, Jiang Y. Rheb activates mTOR by antagonizing its endogenous inhibitor, FKBP38. *Science* 2007;318:977–980
36. Fingar DC, Salama S, Tsou C, Harlow E, Blenis J. Mammalian cell size is controlled by mTOR and its downstream targets S6K1 and 4EBP1/eIF4E. *Genes Dev* 2002;16:1472–1487
37. Haruta T, Uno T, Kawahara J, Takano A, Egawa K, Sharma PM, Olefsky JM, Kobayashi M. A rapamycin-sensitive pathway down-regulates insulin signaling via phosphorylation and proteasomal degradation of insulin receptor substrate-1. *Mol Endocrinol* 2000;14:783–794
38. Rui L, Fisher TL, Thomas J, White MF. Regulation of insulin/insulin-like growth factor-1 signaling by proteasome-mediated degradation of insulin receptor substrate-2. *J Biol Chem* 2001;276:40362–40367
39. Shah OJ, Wang Z, Hunter T. Inappropriate activation of the TSC/Rheb/mTOR/S6K cassette induces IRS1/2 depletion, insulin resistance, and cell survival deficiencies. *Curr Biol* 2004;14:1650–1656
40. Harrington LS, Findlay GM, Gray A, Tolkacheva T, Wigfield S, Rebholz H, Barnett J, Leslie NR, Cheng S, Shepherd PR, Gout I, Downes CP, Lamb RF. The TSC1–2 tumor suppressor controls insulin-PI3K signaling via regulation of IRS proteins. *J Cell Biol* 2004;166:213–223
41. Briaud I, Dickson LM, Lingohr MK, McCuaig JF, Lawrence JC, Rhodes CJ. Insulin receptor substrate-2 proteasomal degradation mediated by a mammalian target of rapamycin (mTOR)-induced negative feedback down-regulates protein kinase B-mediated signaling pathway in β -cells. *J Biol Chem* 2005;280:2282–2293
42. Ozcan U, Ozcan L, Yilmaz E, Duvel K, Sahin M, Manning BD, Hotamisligil GS. Loss of the tuberous sclerosis complex tumor suppressors triggers the unfolded protein response to regulate insulin signaling and apoptosis. *Mol Cell* 2008;29:541–551
43. Shigeyama Y, Kobayashi T, Kido Y, Hashimoto N, Asahara S, Matsuda T, Takeda A, Inoue T, Shibutani Y, Koyanagi M, Uchida T, Inoue M, Hino O, Kasuga M, Noda T. Biphasic response of pancreatic beta-cell mass to ablation of tuberous sclerosis complex 2 in mice. *Mol Cell Biol* 2008;28:2971–2979
44. Hennige AM, Burks DJ, Ozcan U, Kulkarni RN, Ye J, Park S, Schubert M, Fisher TL, Dow MA, Leshan R, Zakaria M, Mossa-Basha M, White MF. Upregulation of insulin receptor substrate-2 in pancreatic β -cells prevents diabetes. *J Clin Invest* 2003;112:1521–1532
45. Uchida T, Nakamura T, Hashimoto N, Matsuda T, Kotani K, Sakaue H, Kido Y, Hayashi Y, Nakayama KI, White MF, Kasuga M. Deletion of *Cdkn1b* ameliorates hyperglycemia by maintaining compensatory hyperinsulinemia in diabetic mice. *Nat Med* 2005;11:175–182
46. Im E, von Lintig FC, Chen J, Zhuang S, Qui W, Chowdhury S, Worley PF, Boss GR, Pilz RB. Rheb is in a high activation state and inhibits B-Raf kinase in mammalian cells. *Oncogene* 2002;21:6356–6365
47. Karbowiczek M, Cash T, Cheung M, Robertson GP, Astrinidis A, Henske EP. Regulation of B-Raf kinase activity by tuberin and Rheb is mammalian target of rapamycin (mTOR) independent. *J Biol Chem* 2004;279:29930–29937
48. Karbowiczek M, Robertson GP, Henske EP. Rheb inhibits C-Raf and B-Raf/C-Raf heterodimerization. *J Biol Chem* 2006;281:25447–25456